

Synthesis, Structure, and Luminescent Properties of Guanidinate-Based Terbium Complexes

Xingan Pang,^[a] Hongmei Sun,^[a] Yong Zhang,^[a] Qi Shen,^{*,[a,b]} and Hongjie Zhang^[c]

Keywords: Terbium complex / Guanidinate / Luminescence / Lanthanides

Two guanidinate-based terbium complexes $[iPrNC(NiPr_2)NiPr]_mTbCl_{3-m}$ [$m = 3$ (**1**), 2 (**2**)] were synthesized, and the crystal structure of **1** was determined by single-crystal X-ray diffraction. Complexes **1** and **2** were further characterized by elemental analysis, IR, and 1H NMR spectroscopy. In complex **1** the guanidinate ligand coordinates to the terbium atom through the nitrogen atoms in a bidentate chelating coordination mode. As a result of an efficient energy transfer

from the guanidinate ligand to the central Tb^{3+} , both **1** and **2** have been found to exhibit strong green emission corresponding to $Tb^{3+} \ ^5D_4 \rightarrow ^7F_J$ ($J = 6, 5, 4, 3$) transitions. Among them, the emission $^5D_4 \rightarrow ^7F_5$ (550 nm) is the most prominent. The lifetimes of the 5D_4 Tb^{3+} excited levels of the two complexes were determined to be around 0.90 ms.

(© Wiley-VCH Verlag GmbH & Co. KGaA, 69451 Weinheim, Germany, 2005)

Introduction

The luminescence properties of lanthanide ions (i.e., narrow emission peak, high quantum yield, and long decay time), in particular Tb^{3+} and Eu^{3+} , make them useful in luminescence probes for chemical or biological systems.^[1] The strong luminescence of lanthanide complexes depends on the energy-level structure of the ligands and the central metal ions. Therefore, considerable efforts have been made to design and assemble lanthanide complexes with organic ligands such as β -diketones,^[2] cryptands,^[3] aromatic carboxylic acids,^[4] and heterocyclics^[5]. Lately, guanidinate anions, $[(RN)_2CNR']_2^-$, whose steric and electronic effects can be easily modified by the variation of substituents on the N-atoms, have attracted considerable attention in organometallic chemistry,^[6] and their application in organolanthanide complexes has led to the synthesis of a series of guanidinate derivatives of lanthanides.^[6–14] Moreover, these complexes with guanidinate as the auxiliary ligands have many uses in catalytic chemistry. For example, the guanidinate aryloxy lanthanum complex can act as the catalyst for the ring-opening polymerization of lactide.^[10] The guanidinate–methyl complexes of lanthanides are effective initiators not only for the polymerizations of MMA and ϵ -capro-

lactone,^[11] but also for styrene polymerization.^[12] The homoleptic triguanidinate lanthanides can also efficiently initiate the ring-opening polymerization of ϵ -caprolactone^[14] and cyclocarbonate.^[15] However, to our best knowledge, the photophysical properties of the guanidinate derivatives of lanthanides still remain unexplored. More recently, our group found that the Tb complex with β -diketiminato as a ligand showed a strong green emission band due to an efficient energy transfer from the β -diketiminato to the central Tb^{3+} .^[16] Considering the similar structural characteristics of guanidinate and β -diketiminato, it is interesting to investigate the photoluminescence behavior of the guanidinate complex of lanthanides. Accordingly, two guanidinate complexes of terbium $\{[iPrNC(NiPr_2)NiPr]_mTbCl_{3-m}, m = 3$ (**1**), 2 (**2**)\} were synthesized and their luminescence spectra were determined. Both of them exhibited strong green emission corresponding to $Tb^{3+} \ ^5D_4 \rightarrow ^7F_J$ ($J = 6, 5, 4, 3$) transitions. Herein, we would like to report the results.

Results and Discussion

Synthesis of $[iPrNC(NiPr_2)NiPr]_mTbCl_{3-m}$ [$m = 3$ (**1**), 2 (**2**)]

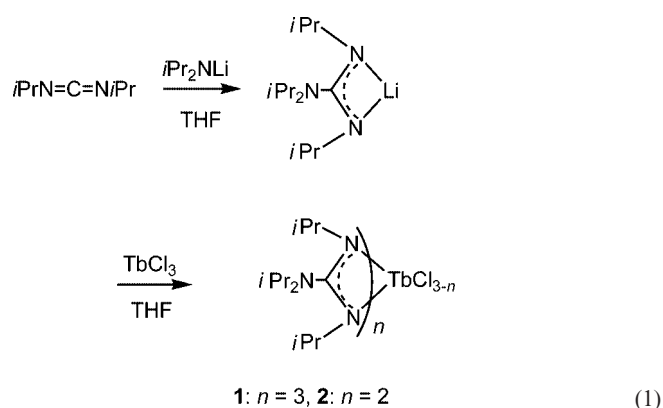
The complexes **1** and **2** can be easily synthesized by the reaction of freshly-prepared lithium guanidinate with $TbCl_3$. The reaction of $TbCl_3$ with lithium guanidinate in 1:3 and 1:2 mole ratios, respectively, after work up at room temperature, gave the two expected complexes as white crystals [Equation (1)]. The complexes are air- and moisture-sensitive and soluble in THF, diethyl ether, and toluene. The initial characterization of complexes **1** and **2** were supported by elemental analysis and IR spectroscopy. In their IR spectra, no signal of $C=N=C$ near 2110 cm^{-1} was ob-

[a] Department of Chemistry and Chemical Engineering, Suzhou University, Suzhou 215006, China
Fax: +86-512-65112371
E-mail: qshen@suda.edu.cn

[b] State Key Laboratory of Organometallic Chemistry, Shanghai Institute of Organic Chemistry, Chinese Academy of Sciences, Shanghai 200032, China

[c] Key Laboratory of Rare Earth Chemistry and Physics, Changchun Institute of Applied Chemistry, Chinese Academy of Sciences, Changchun 130022, China

served, and a strong absorption at approximately 1640 cm^{-1} assigned to the C=N stretch appeared. The IR data indicated that the electrons within the double bonds of the N–C–N linkage are delocalized in the two complexes



Crystal-Structure Analysis of Complex 1

Crystals of complex **1** suitable for X-ray crystallographic analysis were obtained by recrystallization from THF solution at $-15\text{ }^{\circ}\text{C}$. The crystal-structure analyses revealed that complex **1** is a monomer in the solid state. Figure 1 depicts the molecular structure of complex **1**. Selected bond lengths and angles are given in Table 1. The terbium ion in the complex is coordinated to six nitrogen atoms of the three bidentate guanidinate anions and the geometry around the center metal can be best described as a distorted octahedron. The sum of the three angles C(1)–Tb(1)–C(14) [$119.36(19)^{\circ}$], C(14)–Tb(1)–C(27) [$120.8(2)^{\circ}$], and C(27)–Tb(1)–C(1) [$119.87(19)^{\circ}$] equals 360.03° , which indicates that the terbium ion is located in a plane defined by the three central carbon atoms of the guanidinate moieties. All of the C–N bond lengths for the N–C–N moiety of each guanidinate

group are intermediate between the C–N and C=N bond lengths. The results indicated the delocalization of the π bond in the N–C–N unit, while the C(1)–N(3), C(14)–N(6), and C(27)–N(9) bond lengths are $1.452(10)$, $1.411(9)$, and $1.422(9)$, respectively; these values fall into the normal C–N single bond-length range. The Tb–N bond lengths range from 2.380 \AA to 2.411 \AA . The average Tb–N bond length (2.393 \AA) is comparable to those for $[(i\text{PrN})_2\text{CNiPr}_2]_3\text{Nd}$ (2.464 \AA) and $[(\text{CyN})_2\text{CNiPr}_2]_3\text{Nd}$ (2.458 \AA)^[14] when the difference in the ionic radii of Nd and Tb is considered. The angles of the three N–C–N units are slightly different, ranging from $114.0(6)^{\circ}$ to $117.2(7)^{\circ}$, which are also comparable to those for $[(i\text{PrN})_2\text{CNiPr}_2]_3\text{Nd}$ (115°) and $[(\text{CyN})_2\text{CNiPr}_2]_3\text{Nd}$ (114°). The N–Tb–N angle in each TbN_2C moiety is about 56.4° , which is slightly larger than that in the analogous complexes of $[(\text{CyN})_2\text{CNiPr}_2]_3\text{Nd}$ (54.5°) and $[(i\text{PrN})_2\text{CNiPr}_2]_3\text{Nd}$ (54.2°).

Table 1. Selected bond lengths [\AA] and angles [$^{\circ}$] for **1**.

Tb(1)–N(1)	2.382(6)	Tb(1)–N(2)	2.411(6)
Tb(1)–N(4)	2.380(6)	Tb(1)–N(5)	2.392(6)
Tb(1)–N(7)	2.393(6)	Tb(1)–N(8)	2.402(6)
Tb(1)–C(1)	2.803(8)	Tb(1)–C(14)	2.836(7)
Tb(1)–C(27)	2.832(7)	N(1)–C(1)	1.318(9)
N(2)–C(1)	1.333(10)	N(3)–C(1)	1.452(10)
N(4)–C(14)	1.355(10)	N(5)–C(14)	1.343(10)
N(6)–C(14)	1.411(9)	N(7)–C(27)	1.342(9)
N(8)–C(27)	1.335(10)	N(9)–C(27)	1.422(9)
N(1)–Tb(1)–N(2)	56.4(2)	N(4)–Tb(1)–N(5)	56.6(2)
N(7)–Tb(1)–N(8)	56.2(2)	C(1)–Tb(1)–C(27)	119.87(19)
C(1)–Tb(1)–C(14)	119.36(19)	C(27)–Tb(1)–C(14)	120.8(2)
N(1)–C(1)–N(2)	117.2(7)	N(5)–C(14)–N(4)	114.0(6)
N(8)–C(27)–N(7)	115.2(6)		

Photoluminescence Properties of Complexes 1 and 2

Figure 2 shows the excitation spectra of complex **1** in the solid state at room temperature (a), in THF solution at 77 K (b), and of complex **2** in the solid state at room temperature (c). The spectra were monitored by the Tb^{3+} green emission at 550 nm ($^5\text{D}_4\text{--}^7\text{F}_5$) and recorded in a range of 200 to 500 nm . The three excitation spectra are very similar and all of them display broad bands: from 230 to 400 nm with a maximum at 345 nm in the solid state at room temperature and at 304 nm in THF at 77 K for complex **1**, and from 250 to 410 nm with a maximum at 355 nm in the solid state for complex **2**. In the excitation spectra of both complexes, determined in the solid state at room temperature (see a and c in Figure 2), there is a shoulder at 488 nm and a broad band from 200 to 410 nm , which can be attributed to the f–f excitation transition ($^7\text{F}_6\text{--}^5\text{D}_4$) within the $\text{Tb}^{3+} 4f^8$ electron configuration.^[17] The wide excitation band observed can be attributed to the $\pi\text{--}\pi^*$ transition of the guanidinate ligand, in accordance with its broad character and strong intensity. Upon excitation into the absorption of the ligand at 345 nm and 350 nm in the solid state at room temperature, for complexes **1** (see a in Figure 3) and **2** (see b in

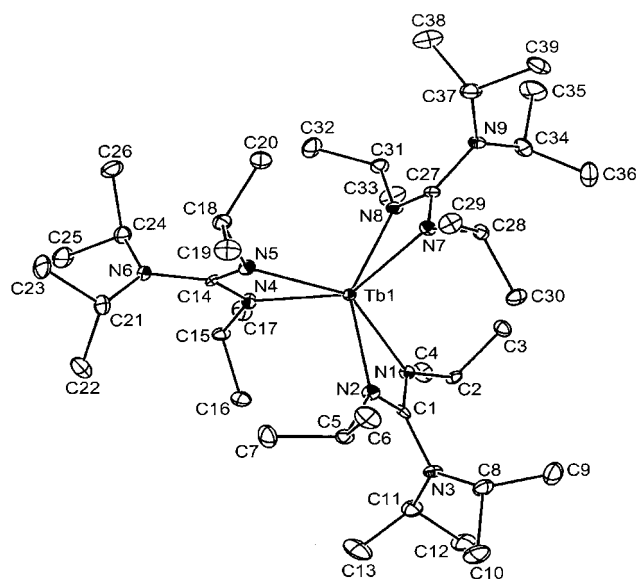


Figure 1. ORTEP diagram of complex **1** (15% thermal ellipsoids).

Figure 3), and at 306 nm in the THF solution at 77 K for complex **1** (Figure 4), almost the same emission spectra were obtained. All of the spectra display strong green luminescence with four emission bands at 485, 546, 585, and 624 nm. The broad band from the ligand in the range of 230 to 410 nm was also not observed. These results indicated that an efficient energy transfer from the guanidinate ligand state to the emitting 5D_4 level of the Tb^{3+} ion occurs. These bands correspond to the characteristic emission from the $^5D_4-^7F_J$ ($J = 6, 5, 4, 3$) transition of the Tb^{3+} ion. Among them the $^5D_4-^7F_5$ transition is the strongest one. The splits of the emission bands corresponding to $^5D_4-^7F_6$, $^5D_4-^7F_5$, and $^5D_4-^7F_4$ are 2, 3, and 4, respectively, which is caused by the crystal field splitting.^[18] We can also see that the emission intensity of complex **1** (see **a** in Figure 3) is stronger than that of complex **2** (see **b** in Figure 3), which shows the number of the ligands affects the luminescent intensity of the guanidinate Tb complexes.

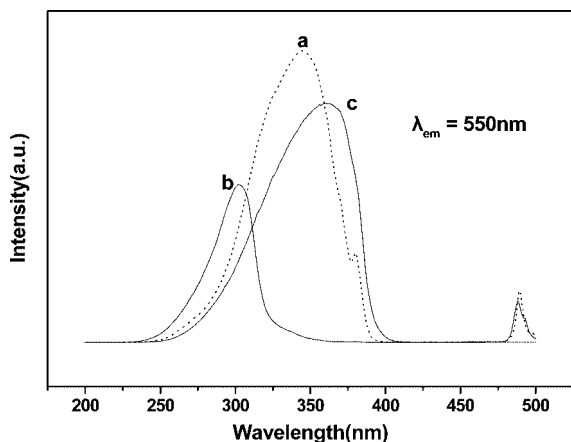


Figure 2. Excitation spectra (a) of complex **1** in the solid state at room temperature; (b) of complex **1** in THF solution at 77 K, and (c) of complex **2** in the solid state at room temperature.

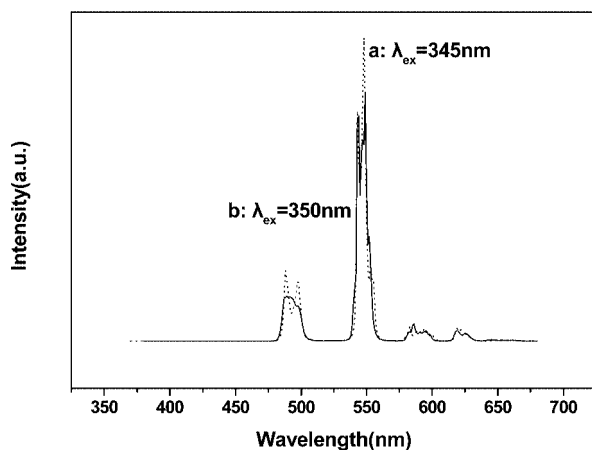


Figure 3. Emission spectra of complexes **1** (a) and **2** (b) in the solid state at room temperature.

The luminescence decay curves of Tb^{3+} ($^5D_4-^7F_5$ at 546 nm) in complex **1** were obtained under different excitation wavelengths at room temperature. The decay curves under the excitation wavelengths 546, 485, and 624 nm are

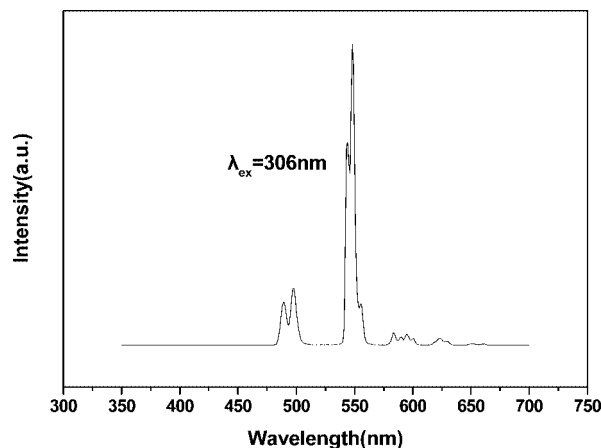


Figure 4. Emission spectrum of complex **1** in THF solution at 77 K.

shown in Figure 5 and Figure 6. It is clear that the luminescence of Tb^{3+} in complex **1** shows simple decay behavior. The decay curves fitted well into a singly exponential function as $I = I_0 \exp(-t/\tau)$ (τ is 1/e lifetime of the rare earth ion), indicating that all the Tb ions occupy the same average local environment. The lifetime of the Tb^{3+} ion (τ) is determined to be 0.91, 0.87, and 0.95 ms for $^5D_4-^7F_5$, $^5D_4-^7F_6$, and $^5D_4-^7F_3$, respectively. This result means that the ligands are efficiently shielding the Tb ion. The lifetime of the 5D_4 Tb^{3+} excited level in complex **2** was determined to be 0.86 ms, as shown in Figure 7. This value is very close to that of complex **1**; evidently, the number of ligands in the complex does not influence the lifetime.

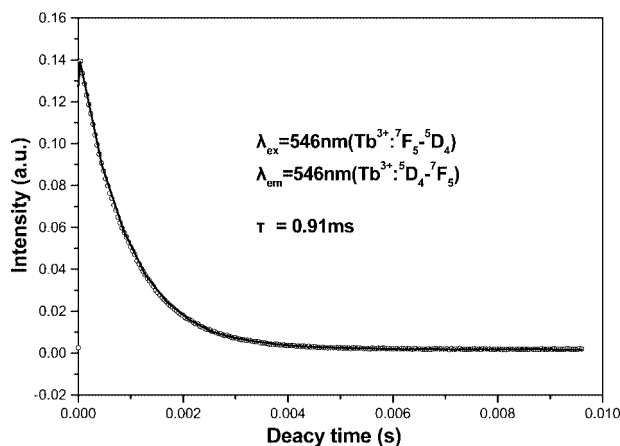


Figure 5. The decay curve for the luminescence of Tb^{3+} in complex **1** under an excitation wavelength of 546 nm.

Conclusions

In summary, bis- and tris-guanidinate terbium complexes can be easily prepared in good yield by the metathesis reaction of lithium guanidinate with anhydrous terbium trichloride at different mole ratios. The structural features of homoleptic terbium guanidinate (**1**) have been determined by X-ray diffraction. Interestingly, both of the two com-

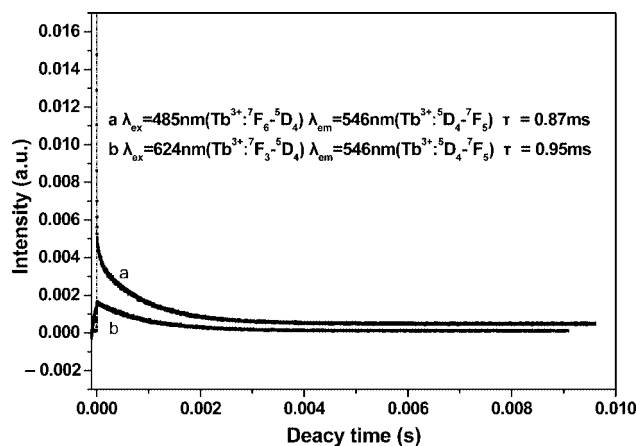


Figure 6. The decay curves for the luminescence of Tb^{3+} in complex **1** under the excitation wavelengths of 485 and 624 nm.

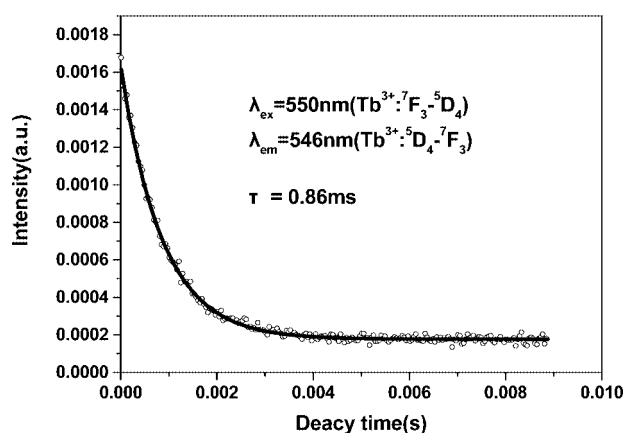


Figure 7. The decay curve for the luminescence of Tb^{3+} in complex **2** under an excitation wavelength of 550 nm.

plexes show rich luminescent properties at room temperature or 77 K. The lifetimes of the $^5\text{D}_4$ Tb^{3+} excited levels of the guanidinate complexes were determined to be around 0.90 ms. These results suggest that guanidinate could be used as a novel type of ligand for the synthesis of lanthanide-based luminescent complexes.

Experimental Section

General Procedures: All manipulations were performed under pure Ar with rigorous exclusion of air and moisture by the standard Schlenk techniques. Solvents were distilled from Na/benzophenone ketyl prior to use. Anhydrous TbCl_3 [19] was prepared according to the literature procedures. *N,N'*-diisopropylcarbodiimide was purchased from Aldrich and purified by distillation under reduced pressure. Metal analyses were carried out by complexometric titration. Carbon, hydrogen, and nitrogen analyses were performed by direct combustion with a Carlo-Erba EA-1110 instrument. The IR spectra were recorded with a Magna-IR 550 spectrometer. ^1H NMR spectra were measured with a Unity Inova-400 spectrometer. The excitation and emission spectra were obtained with a SPEX FL-2T2 spectrofluorimeter with a 0.8 mm slit and equipped with a 450-W lamp as the excitation source. Luminescence lifetimes were measured with a Lecroy Wave Runner 6100 Digital Oscilloscope

(1 GHz) using a 350-nm Ar ion laser (pulse width = 4 ns) as the excitation source (Continuum Sunlite OPO).

Synthesis of $[\text{iPrNC}(\text{iPr}_2\text{N})\text{NiPr}]_3\text{Tb}$ (1**):** A freshly-prepared solution of lithium guanidinate $[(\text{iPrN})_2\text{CNiPr}_2]\text{Li}$ (2.2 g, 10 mmol) in THF (40 mL) was cannula-transferred into a Schlenk tube (100 mL) containing a solution of TbCl_3 (0.88 g, 3.33 mmol) in THF (20 mL) at 0 °C. The reaction mixture was stirred for 20 min at 0 °C and then stirred for 48 h at room temperature. The solvent was removed in vacuo, and the residue was extracted with toluene (45 mL) and LiCl was removed by centrifugation. After the extracts were concentrated and cooled to -15 °C for crystallization, colorless microcrystals were obtained (1.84 g, 66%). ^1H NMR (400 MHz, C_6D_6 , 25 °C): δ = 2.88–3.76 [m, 12 H, $\text{CH}(\text{CH}_3)_2$], 0.68–1.76 [m, 72 H, $\text{CH}(\text{CH}_3)_2$] ppm. $\text{C}_{39}\text{H}_{84}\text{N}_9\text{Tb}$ (838.07): calcd. C 55.89, H 10.08, N 15.03, Tb 19; found: C 55.77, H 10.12, N 14.98, Tb 19.08. IR [KBr pellet (cm^{-1})]: 2969 (s), 2863 (s), 2709 (m), 2617 (m), 1651 (s), 1450 (s), 1361 (s), 1317 (s), 1210 (s), 1058 (s), 1018 (m), 975 (m), 930 (m), 861 (m), 667 (m), 576 (cm^{-1}).

Synthesis of $[\text{iPrNC}(\text{iPr}_2\text{N})\text{NiPr}]_2\text{TbCl}(\text{THF})$ (2**):** Following a procedure similar to the synthesis of **1**, using $[(\text{iPrN})_2\text{CNiPr}_2]\text{Li}$ (1.74 g, 8 mmol), TbCl_3 (1.06 g, 4 mmol), and THF (60 mL), followed by crystallization from THF yielded white crystals (1.72 g, 60%). ^1H NMR (400 MHz, C_6D_6 , 25 °C): δ = 2.80–3.82 [m, 8 H, $\text{CH}(\text{CH}_3)_2$], 0.68–1.80 [m, 48 H, $\text{CH}(\text{CH}_3)_2$] ppm. $\text{C}_{30}\text{H}_{64}\text{N}_6\text{ClO}_2\text{Tb}$ (718.42): calcd. C 50.11, H 8.9, N 11.69, Tb 22.13; found: C 49.98, H 8.86, N 11.98, Tb 22.54. IR [KBr pellet (cm^{-1})]: 2972 (s), 2865 (s), 2612 (s), 2463 (m), 1634 (s), 1473 (s), 1449 (s), 1367 (s), 1322 (s), 1173 (m), 1118 (m), 1014 (m), 922 (m), 866 (m), 809 (m), 722 (m), 661 (cm^{-1}).

X-ray Structural Determination of Complex 1: Suitable single crystals of complex **1** were each sealed in a thin-walled glass capillary, and intensity data were collected with a Rigaku Mercury CCD equipped with graphite-monochromated Mo- $K\alpha$ (λ = 0.7107 Å) radiation. Details of the intensity data collection and crystal data are given in Table 2. The crystal structure was solved by direct methods and expanded by Fourier techniques. Atomic coordinates and ther-

Table 2. Details of the crystallographic data collection and refinement for **1**.

Empirical formula	$\text{C}_{39}\text{H}_{84}\text{N}_9\text{Tb}$
Molecular mass	838.07
Temperature [K]	298(2)
Wavelength [Å]	0.71070
Size [mm]	$0.80 \times 0.79 \times 0.45$
Crystal system	triclinic
Space group	$P\bar{1}$
<i>a</i> [Å]	13.3839(8)
<i>b</i> [Å]	13.3968(9)
<i>c</i> [Å]	18.0812(2)
α [°]	70.27(2)
β [°]	74.38(2)
γ [°]	59.69(2)
<i>V</i> [Å ³]	2614.9(6)
<i>Z</i> [Å ³]	2
<i>D</i> _{calc.} [g/mL]	1.064
Absorption coefficient (mm^{-1})	1.383
<i>F</i> (000)	892
Theta range for collection [°]	3.06–27.48
Reflection collected	25056
Independent reflections	11382
<i>R</i> [<i>I</i> > 2σ(<i>I</i>)]	0.1943
<i>R</i> _w	0.1957
Goodness-of-fit on <i>F</i> ²	1.252

mal parameters were refined by full-matrix least-squares analysis on F^2 . All non-hydrogen atoms were refined anisotropically. Hydrogen atoms were all generated geometrically with assigned appropriate isotropic thermal parameters. CCDC-245779 (for **1**) contains the supplementary crystallographic data for this paper. These data can be obtained free of charge from The Cambridge Crystallographic Data Centre via www.ccdc.cam.ac.uk/data_request/cif.

Acknowledgments

We are indebted to the Chinese National Natural Science Foundation.

- [1] G. F. de Sá, O. L. Malta, C. de Mello Donegá, A. M. Simas, R. L. Longo, P. A. Santa-Cruz, E. F. da Silva Jr., *Coord. Chem. Rev.* **2000**, *196*, 165.
- [2] H. G. Liu, S. Park, K. Jang, X. S. Feng, C. Kim, H. J. Seoe, Y. I. Lee, *J. Lumin.* **2004**, *106*, 47.
- [3] S. Faulkner, A. Beeby, M.-C. Carrié, A. Dadabhoy, A. M. Kenwright, P. G. Sammes, *Inorg. Chem. Commun.* **2001**, *4*, 187.
- [4] M. C. Yin, C. C. Ai, L. J. Yuan, J. T. Sun, *J. Mol. Struct.* **2004**, *691*, 33.
- [5] M. Pietraszkiewicz, J. Karpiuk, O. Pietraszkiewicz, *J. Alloys Compd.* **2000**, *300–301*, 141.
- [6] P. J. Bailey, S. Pace, *Coord. Chem. Rev.* **2001**, *214*, 91.
- [7] Y. L. Zhou, G. P. A. Yap, D. S. Richeson, *Organometallics* **1998**, *17*, 4387.
- [8] Z. Lu, G. P. A. Yap, D. S. Richeson, *Organometallics* **2001**, *20*, 706.
- [9] J. Zhang, R. F. Cai, L. H. Weng, X. G. Zhou, *J. Organomet. Chem.* **2003**, *672*, 94.
- [10] G. R. Giesbrecht, G. D. Whitener, J. Arnold, *J. Chem. Soc. Dalton Trans.* **2001**, 923.
- [11] Y. J. Luo, Y. M. Yao, Q. Shen, K. B. Yu, L. H. Weng, *Eur. J. Inorg. Chem.* **2003**, 318.
- [12] Y. J. Luo, Y. M. Yao, Q. Shen, *Macromolecules* **2002**, *35*, 8670.
- [13] Y. M. Yao, Y. J. Luo, J. L. Chen, Z. Q. Zhang, Y. Zhang, Q. Shen, *J. Organomet. Chem.* **2003**, *679*, 229.
- [14] J. L. Chen, Y. J. Luo, Y. M. Yao, L. Y. Zhou, Y. Zhang, Q. Shen, *J. Organomet. Chem.* **2004**, *689*, 1019.
- [15] L. Y. Zhou, Y. M. Yao, Y. Zhang, M. Q. Xue, J. L. Chen, Q. Shen, *Eur. J. Inorg. Chem.* **2004**, 2167.
- [16] Z. Q. Zhang, Q. Shen, Y. Zhang, Y. M. Yao, J. Lin, *Inorg. Chem. Commun.* **2004**, *7*, 305.
- [17] G. Blasse, B. C. Grabmaier, *Luminescent Materials*, Springer, Berlin, Heidelberg, **1994**.
- [18] K. B. Yatsimirski, N. K. Davidenko, *Coord. Chem. Rev.* **1979**, *27*, 223.
- [19] M. D. Taylor, C. P. Carter, *J. Inorg. Nucl. Chem.* **1962**, *24*, 387.

Received: September 10, 2004